

Employment of encapsulated Si with mesoporous TiO₂ layer as anode material for lithium secondary batteries

Sang-Eun PARK¹, Bo-Eun KIM¹, Sang-Wha LEE², Joong-Kee LEE¹

1. Advanced Energy Materials Processing Laboratory, Korea Institute of Science and Technology,
P. O. Box 131, Cheongryang, Seoul, 130-650, Korea;

2. Department of Chemical & Bio Engineering, Kyungwon University, San 65 Bokjeong-Dong, Sujeong-Ku,
Seongnam, Gyeonggi-Do, 461-701, Korea

Received 18 June 2008; accepted 10 March 2009

Abstract: Silicon composite of nano-capsule type is newly applied as an active anode material for lithium ion batteries. TiO₂-encapsulated silicon powders were synthesized by a sol-gel reaction with titanium ethoxide. Silicon nanoparticles were successfully embedded into porous titanium oxide capsules that played as a buffer layer against drastic volume changes of silicon during the charge-discharge cycling, consequently leading to the retardation of the capacity fading of intrinsic silicon materials. The electrochemical and structural properties of silicon nanocomposites with different surface areas of encapsulating TiO₂ layer were characterized by X-ray diffraction(XRD), nitrogen gas adsorption analysis by the Brunauer-Emmett-Teller(BET) equation, transmission electron microscopy(TEM), and galvanostatic charge-discharge experiments.

Key words: sol-gel, TiO₂, silicon, secondary battery

1 Introduction

Silicon has been considered one of the most promising candidates as an anode material for lithium ion batteries because it has much higher energy density (4 200 mA·h/g) in comparison with that of commercialized graphite (372 mA·h/g). However, there are some disadvantages to apply silicon for anode materials of lithium ion batteries. The major obstacle to overcome is the mechanical failure by the repeated large volume expansion related to alloying with lithium ions during the charge-discharge cycling[1].

There have been many attempts to overcome the large volume expansion of silicon anode materials by the preparation of nanosized Si[2–3], Si-based thin film [4–6], and Si-based composite anodes[7–10]. The cyclic stability of nanoscaled Si and Si-based thin film anodes was improved probably due to the reduced density of atoms in a nanosized grain and/or the enhanced fracture mechanism of Si nanoparticles[11–12]. Silicon composites with an inactive matrix (such as TiN and TiB₂) and/or an active carbon matrix in which silicon is finely dispersed also showed an improved cyclic

stability.

Recently, Si-dispersed ZrO₂ film was fabricated by using sol-gel and dipping method[13]. A mesoporous ZrO₂ composite films can not only improve the transferring of ions and reduce the diffusion resistance of anode, but also assuage the volume expansion of anode materials. Sol-gel method can provide a facile synthetic route for producing oxide composites. Compared with the conventional techniques such as flame or plasma-induced decomposition methods, the sol-gel process has several advantages in the fabrication of non-metallic and inorganic solid materials, e.g., considerably low working temperature and facile production of porous films and bulk materials with various shapes[14].

In this study, silicon nanopowder was encapsulated by a mesoporous TiO₂ layer which can play a buffer layer and a dispersion matrix of silicon nanoparticles. Sol-gel reaction of continuous hydrolysis and condensation of metal alkoxides finally form a three-dimensionally polymeric network, i.e., encapsulation of silicon nanoparticles with mesoporous TiO₂ layer. Some factors that affect the sol-gel reaction include type of precursor, type of solvent, water contents, acid (or base)

contents, precursor concentration, temperature, and so forth. In particular, the electrochemical characteristics of TiO_2 -encapsulated Si were systematically investigated with the variation of molar ratio of H_2O to precursor, R , in the presence of 0.014 mol/L ammonium hydroxide (28%, mass fraction) as a basic catalyst.

2 Experimental

2.1 Preparation of anode material

For TiO_2 coating, silicon nanoparticles (Alfa Aesar, 50–100 nm) were dispersed in ethanol under ultrasound irradiation. Certain amounts of distilled water and ammonium hydroxide were added to the mixture solution with magnetic stirring. Titanium ethoxide (TEOT) dissolved in absolute ethanol was slowly added into the mixture solution, followed by further stirring for 30 min. The molar ratio of water to TEOT was determined based on the final concentrations of water and TEOT after the addition of TEOT. TiO_2 -coated silicon nanoparticles (Si@TiO_2) were centrifuged and purified several times to remove impurities. The collected Si@TiO_2 particles were dried and stored at room temperature.

2.2 Fabrication of half cell

The half-cell electrodes for lithium ion batteries were prepared with the Si nanocomposites prepared in different conditions. For preparing the Si@TiO_2 anode, a slurry containing 70% Si@TiO_2 powder, 15% Denka black(DB) and 15% polyvinylidene fluoride(PVDF) dissolved in N-methyl-2-pyrrolidone(NMP) was pasted onto a 12 μm -thick Cu foil substrate. Half-cells were assembled in a dry room with Si@TiO_2 anode as a working electrode, a metallic lithium foil as the counter electrode, 1 mol/L LiPF_6 in ethylene carbonate (EC), dimethyl carbonate(DMC), and ethymethyl carbonate (EMC) as a electrolyte, and a polypropylene-based film as the separator.

3 Results and discussion

To encapsulate the silicon with porous TiO_2 layer, titanium ethoxide (TEOT) precursor dispersed in ethanol was gradually added into the silicon solution using a syringe pump to suppress the formation of pure TiO_2 particles. Pure TiO_2 nanoparticles that did not react with silicon powder, however, were observed in the final sol-gel products. The slow addition of precursors in reacting sol-gel solution not only keeps the concentration of hydrolyzed Ti—OH at low value, but also minimizes the nucleation of Ti precursor itself. So, the coating efficiency of TiO_2 layer over silicon can be improved. The feeding rate of TEOT was kept at 36.5 $\mu\text{L}/\text{min}$ by a syringe pump.

The adsorption and desorption isotherms are obtained as plots of the equilibrium amounts of N_2 gas adsorbed on the solid surface as a function of the partial pressure p/p^0 at 77 K. Fig.1 shows the type IV isotherms of Si@TiO_2 with $R=2$ and $R=12$ and their total surface areas are 269 and 201 m^2/g , respectively, as can be seen in Table 1.

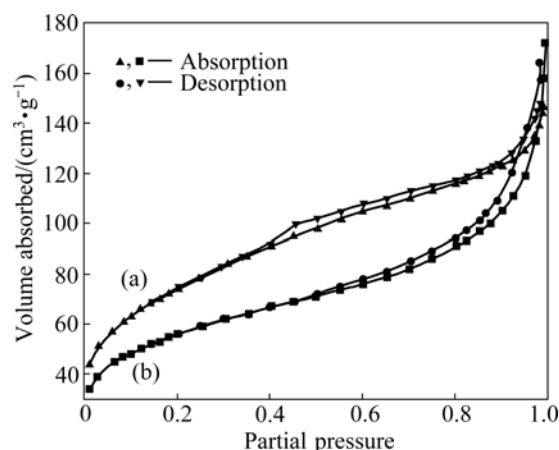


Fig.1 Nitrogen adsorption-desorption isotherms at 77 K of Si@TiO_2 prepared with $R=2$ (a) and 12 (b)

Table 1 Structural and electrochemical characteristics of TiO_2 -encapsulated Si with variation of molar ratio of H_2O to precursor

Condition	Surface area/ ($\text{m}^2\cdot\text{g}^{-1}$)	Average pore diameter/ \AA	Initial efficiency ^a / %	Capacity retention ^b / %
Si	10	—	62.5	0.49
$R=2$	269	31	63	0.76
$R=4$	259	31	75	0.82
$R=12$	201	40	35	0.28

a: Initial efficiency is calculated from discharge capacity over charge capacity at first cycle; b: Capacity retention is calculated from discharge capacity with first cycle over discharge capacity with second cycle.

A characteristic feature of type IV isotherms is the hysteresis that is normally attributed to the existence of pore cavities[15]. Compared with Si@TiO_2 particles with $R=2$, Si@TiO_2 particles with $R=12$ exhibit the low adsorption values at low relative pressures and sudden increase of adsorption values at high pressures. Because the amount of water affects the kinetics of hydrolysis in sol-gel reaction, the low amount of water ($R=2$) lowers the hydrolysis reaction and condensation rate. However, the excess water ($R=12$) causes the excess formation of Ti—OH species and suppresses the development of well-organized Ti—O—Ti chains, consequently leading to loosely packed TiO_2 network. Furthermore, the shrinkage and collapse of this network during a drying process decrease the surface area and pore volume, owing to the effects ascribed to the rigidity and capillary

pressure of mesoporous structure[16].

TEM images of intrinsic Si and Si@TiO₂ nanoparticles with $R=2$ and $R=12$ are shown in Fig.2. The size of Si nanoparticles ranges from 60 to 120 nm with spherical shape. However, almost all particles are aggregated each other. Si nanoparticles are encapsulated by mesoporous TiO₂ layer (about 7 nm in thickness) via sol-gel reaction at $R=2$. With the increase of water content, the surface texture of TiO₂ layer becomes coarser, which seems probable due to the collapse and

shrinkage of the TiO₂ network.

Fig.3 exhibits XRD patterns of the TiO₂-coated Si nanoparticles prepared by the sol-gel method, followed by heat treatment at 873 K under flowing argon for 3 h. Major three peaks of silicon at 28.5°, 47.4°, and 56.2°, corresponds to (111), (220), and (311) planes, respectively. TiO₂-coated silicon nanoparticles without heat treatment do not exhibit a significant peak related to pure TiO₂ phase, as shown in Fig.3(a). Anatase and rutile phases of TiO₂ are observed after heat treatment at 873 K, indicating the existence of predominant amorphous structure of sol-gel derived TiO₂ layer.

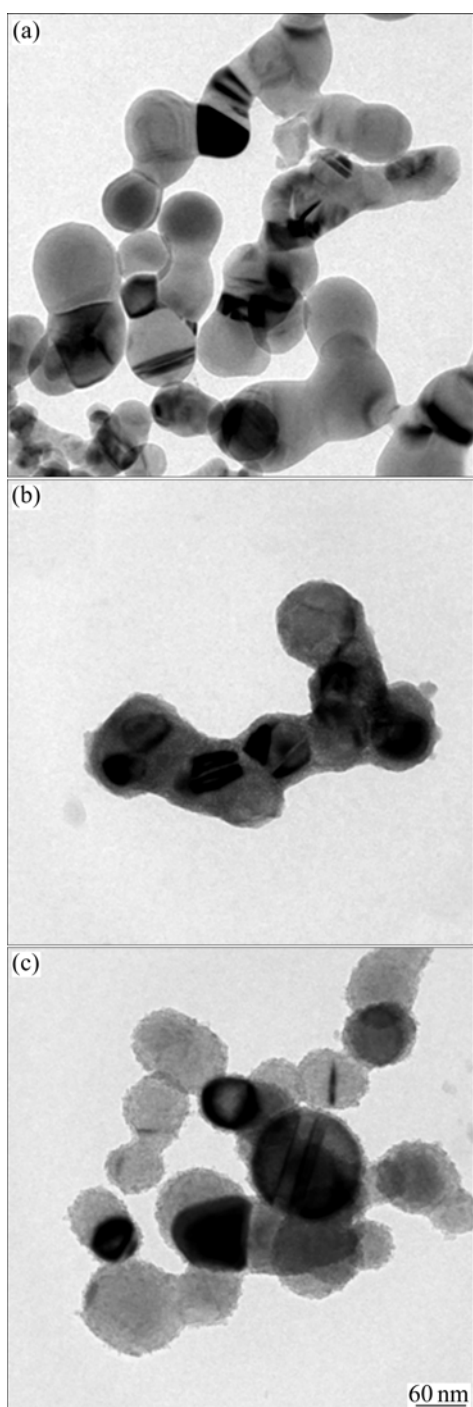


Fig.2 TEM images of intrinsic Si (a), Si@TiO₂ prepared with $R=2$ (b) and 12 (c)

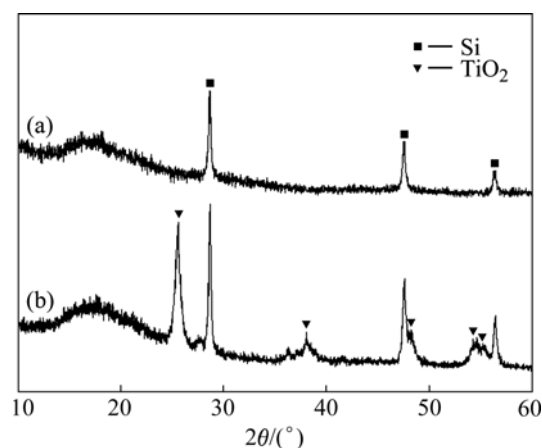


Fig.3 XRD patterns of TiO₂-coated silicon before (a) and after heat treatment at 873 K (b)

Fig.4 shows the electrochemical performance of intrinsic Si and Si@TiO₂ nanoparticles during the charging-discharging cycles. The anode of intrinsic Si exhibits a rapid capacity fading and retains only 49% of initial capacity at the second cycle as shown in Fig.4(a). In the case of the anode of Si@TiO₂ nanoparticles with $R=2$, the discharge capacity still retains 76% of its initial capacity as shown in Fig.4(b). The mesoporous structure of TiO₂ assuages the volume change of Si as a buffering

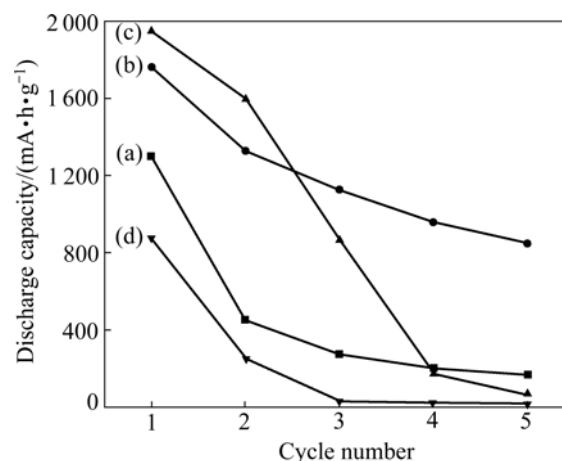


Fig.4 Comparison of cycle performance for intrinsic Si (a) and Si@TiO₂ nanoparticles with $R=2$ (b), 4 (c), and 12 (d)

layer and results in the improvement of cyclic performance. Besides, this kind of mesoporous structure can not only offer convenient channel for the insertion and extraction of lithium ions but also enhance the contact between Si nanoparticles and the electrolytes [13]. However, the capacity retention is sharply decreased with the increase of water content in the sol-gel reaction. The experimental results indicate that the shrinkage and collapse of loosely developed TiO_2 structure negatively affects the cyclic performance of silicon anode.

4 Conclusions

1) Silicon nanoparticles were successfully encapsulated with mesoporous TiO_2 layers through the sol-gel reaction.

2) The surface area and average pore size of Si@TiO_2 particles are affected by the molar ratio of H_2O to TEOT.

3) Low concentration of H_2O ($R=2$) induces a well-developed mesoporous network that obviously plays a buffer layer against the volume expansion of silicon anode. However, high concentration of H_2O ($R=12$) induces a loosely packed mesoporous network due to relatively rapid hydrolysis and condensation rates, consequently leading to the shrinkage and collapse of coating TiO_2 layer.

4) Conclusively, the physical structure of porous TiO_2 layer can be controlled by the hydrolysis and condensation rate, resulting in a different buffering effect against drastic volume change of silicon anode. But it should be noted that there is some possibility of worse effect if the molar ratio of water to precursor is much smaller than 2.

References

- [1] ZENG Z Y, TU J P, WANG X L, ZHAO X B. Electrochemical properties of $\text{Si/LiTi}_2\text{O}_4$ nanocomposite as anode materials for Li-ion secondary batteries [J]. *J Electroanal Chem*, 2008, 616: 7–13.
- [2] GUO Z P, WANG J Z, LIU H K, DOU S X. Study of silicon/polypyrrole composite as anode materials for Li-ion batteries [J]. *J Power Sources*, 2005, 146: 448–451.
- [3] LI H, HUANG X, CHEN L, WU Z, LIANG Y. A high capacity nano-Si composite anode material for lithium rechargeable batteries [J]. *Electrochem Solid-State Lett*, 1999, 2: 547–549.
- [4] GRAETZ J, AHN C C, YAZAMI R, FULTZ B. Highly reversible lithium storage in nanostructured silicon [J]. *Electrochem Solid-State Lett*, 2003, 6: A194–A197.
- [5] JUNG H, PARK M, YOON Y G, KIM G B, JOO S K. Amorphous silicon anode for lithium-ion rechargeable batteries [J]. *J Power Sources*, 2003, 115: 346–351.
- [6] UEHARA M, SUZUKI J, TAMURA K, SEKINE K, TAKAMURA T. Thick vacuum deposited silicon films suitable for the anode of Li-ion battery [J]. *J Power Sources*, 2005, 146: 441–444.
- [7] KIM I S, KUMTA P N, BLOMGREN G S. Si/TiN nanocomposites novel anode materials for Li-ion batteries [J]. *Electrochem Solid-State Lett*, 2000, 3: 493–496.
- [8] KIM B C, UONO H, SATO T, FUSE T, ISHIIHARA T, SENNA M. Li-ion battery anode properties of Si-carbon nanocomposites fabricated by high energy multiring-type mill [J]. *Solid State Ionics*, 2004, 172: 33–37.
- [9] KIM J H, KIM H, SOHN H J. Addition of Cu for carbon coated Si-based composites as anode materials for lithium-ion batteries [J]. *Electrochem Commun*, 2005, 7: 557–561.
- [10] WANG C S, WU G T, ZHANG X B, QI Z F, LI W Z. Lithium insertion in carbon-silicon composite materials produced by mechanical milling [J]. *J Electrochem Soc*, 1998, 145: 2751–2758.
- [11] SURYANARAYANA C. Mechanical alloying and milling [J]. *Prog Mater Sci*, 2001, 45: 1–184.
- [12] WANG G X, AHN J H, YAO J. Nanostructured Si-C composite anodes for lithium-ion batteries [J]. *Electrochem Commun*, 2004, 6: 689–692.
- [13] SHI D Q, TU J P, YUAN Y F, WU H M, LI Y, ZHAO X B. Preparation and electrochemical properties of mesoporous Si/ZrO_2 nanocomposite film as anode material for lithium ion battery [J]. *Electrochem Commun*, 2006, 8: 1610–1614.
- [14] WRIGHT J D, SOMMERDIJK N A J M. Sol-gel materials chemistry and applications [M]. Amsterdam: Gordon and Breach Science Publishers, 2001: 43.
- [15] BRINKER C J, SCHERER G W. Sol-gel science [M]. San Diego: Academic Press, 1990: 523–525.
- [16] WARD D A, KO E I. Preparing catalytic materials by the sol-gel method [J]. *Ind Eng Chem Res*, 1995, 34: 421–433.

(Edited by YANG Hua)